XMM-Newton CCF Release Note

XMM-CAL-SRN-0318

Refinement of the EPIC-MOS Quantum Efficiency at the Silicon edge

Steve Sembay (LUX), Matteo Guainazzi, Richard Saxton, Martin Stuhlinger (ESAC)

30 September 2014

1 CCF components

Name of CCF	VALDATE	EVALDATE	Blocks changed	XSCS flag
EMOS1_QUANTUMEF_0020.CCF	2000-01-01T00:00:00	2002-11-08T00:00:00	QE_TOTAL	NO
EMOS1_QUANTUMEF_0021.CCF	2002-11-08T00:00:01		QE_TOTAL	NO
EMOS2_QUANTUMEF_0020.CCF	2000-01-01T00:00:00	2002-11-08T00:00:00	QE_TOTAL	NO
EMOS2_QUANTUMEF_0021.CCF	2002-11-08T00:00:01		QE_TOTAL	NO

Read et al. (2014) report on a prominent emission-like feature in the EPIC-MOS spectra of bright, non piled-up 2XMM sources. This feature is not present in the simultaneous EPIC-pn spectra of the same sample. These authors suggest that this feature (or, at least, the bulk thereof) could be due to residual inaccuracies of the calibration of the EPIC-MOS cameras effective area at the Silicon photoelectric absorption edge, where it undergoes a local steep gradient.

This Release Note describes an empirical recalibration of the EPIC-MOS Quantum Efficiency CCF constituents primarily driven by these experimental results.

2 Changes

The empirical recalibration was derived from an analysis of observations of targets whose spectra are dominated by featureless continua in the energy range of interest. The targets include blazars and the Vela pulsar PSR B0833-45 . A list of the observations is given in Table 1. The data were processed with SAS 13.5 which includes the new MOS contamination model (not included in the original analysis by Read et al., 2014). For each target, two spectra from each MOS camera were extracted filtered by pattern 0 (mono-pixel) only and pattern 0-12 (all valid X-ray) classes. In each case the source extraction region was an annulus or circle chosen to avoid pile-up. The spectra were fit with absorbed powerlaw (or sum of powerlaw) models in the band 0.8 to 4.5 keV and data/model ratio residual values extracted. The residuals were then stacked together according to camera (MOS1 or MOS2), pattern filter and epoch range. A variety of epoch ranges were looked at in order to explore any potential time-dependency. It was noted that the only significant time-dependant effect was a discontinuity of behaviour in the residuals before and after the lowering of the camera CCD operating temperature (from -100°C to -120°C) which was made during orbit 533 in November 2002. Figures 1, 2, 3 and 4 show the pre- and post-cooling stacked data/model residuals for each camera and pattern filter combination. Error bars on individual points are suppressed for clarity. In each case an empirical fit to the residuals was made by fitting two splines above and below the silicon edge. The spline node points used at each energy are shown by the line of larger dots. Similar behaviour is shown by each camera although there are differences in detail between the pattern 0 and pattern 0-12 classes. The physical explanation for the apparent discontinuity in behaviour due to cooling is under investigation. The spline fits were then used to empirically adjust the MOS quantum efficiency for the two pattern classes with `EMOS[1/2]_QUANTUMEF_0021.CCF` and `EMOS[1/2]_QUANTUMEF_0022.CCF` having validity dates appropriate to the pre- and post-cooling epochs respectively. The energy range of the correction was restricted to the range 0.8 to 2.2 keV. Above 2.2 keV the residuals in the data/model values may be dominated by the mirror effective area which is currently undergoing further recalibration investigations.

Target	Observation ID	Orbit	Used in Sect. 4.1
MS 0737.9+7441	0123100101	0063	No
MS 1229.2+6430	0124900101	0082	No
3C 273	0126700801	0096	Yes
PSR B0833-45	0111080201	0180	Yes
3C 273	0136550101	0277	Yes
3C 273	0137551001	0382	No
PKS 2155-304	0124930501	0450	Yes
PKS 2155-304	0124930601	0545	Yes
3C 273	0159960101	0655	Yes
H1426+428	0165770101	0852	Yes
H1426+428	0165770201	0853	Yes
H1426+428	0310190501	1035	Yes
PSR B0833-45	0153951401	1169	No
MKN 205	0401240501	1258	No
PG 1553+113	0656990101	1952	No
3C 273	0414191001	2308	Yes
PKS 2155-304	0411782101	2449	Yes
PG 1553+113	0727780101	2495	No

Table 1: List of observations used in this analysis.

3 Scientific Impact of this Update

The primary goal of the updated CCF constituents is to smooth out spectral residuals in the EPIC-MOS cameras at the energy of the Silicon photoelectric absorption edge ($\simeq$1.845 keV) down to a level consistent with the current relative uncertainties of the effective area calibration ($\leq$2%).

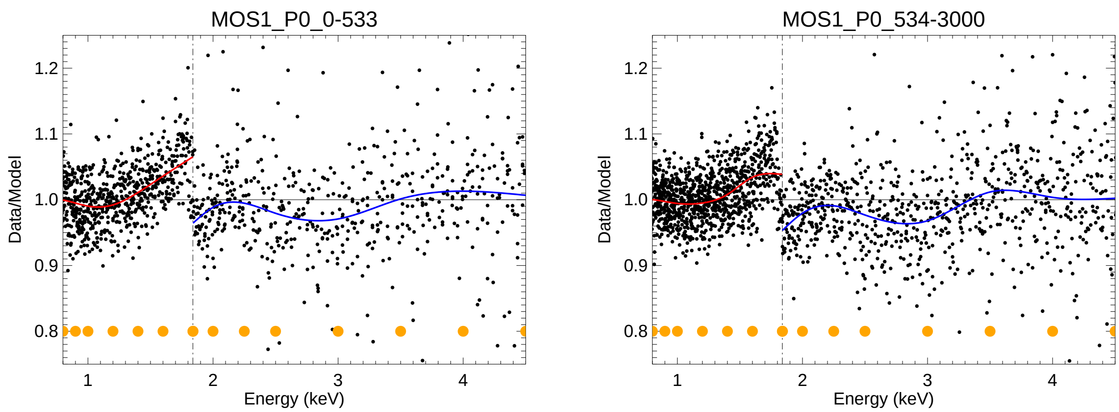

Figure 1: MOS1, pattern 0, pre-cooling (left panel) and post-cooling (right panel) stacked data/model residuals. Spline fits below and above the Si edge (vertical dashed lines) are shown. The line of dots in the lower part of the plots show the chosen positions of the spline knots.

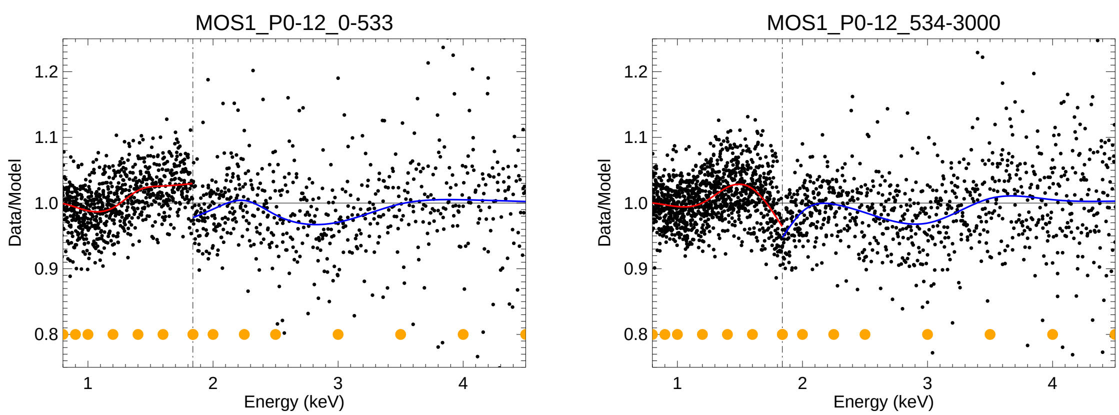

Figure 2: As Figure 1 but for pattern 0-12 selection

4 Estimated Scientific Quality

4.1 Tests on XCAL blazars

In Fig. 5 we show a zoom around the energy of the Silicon edge of the stacked residuals (as defined in Longinotti et al. 2008, and Kettula et al. 2013) obtained on a sample of radio-loud Active Galactic Nuclei in the XMM-Newton cross-calibration (XCAL) database extracted from the observations in Table 1. Details on the data reduction can be found in Stuhlinger et al. (2010). The standard `PATTERN` (0–12) spectrum of each individual source and camera was fit in the 0.3–10 keV energy band with a parabolic power-law model $F(E) = e^{\alpha+\beta\times\log(E)}$ modified by photoelectric absorption (model `phabs` in XSPEC 12.8) with free column density. The dynamical range of the residuals is significantly reduced from $\simeq$6% to $\simeq$2% and from $\simeq$7% to $\simeq$2% in MOS1 and MOS2, respectively. Comparable improvements are obtained on spectra extracted using single events only.

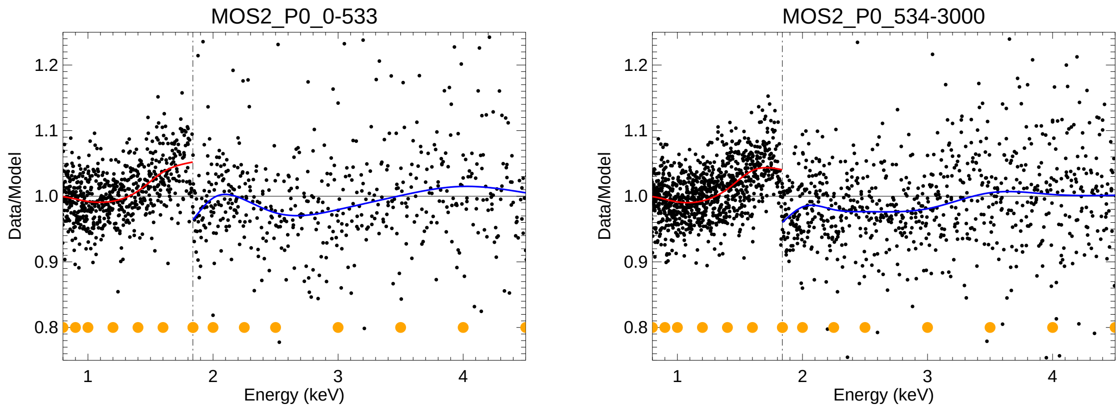

Figure 3: As Figure 1 but for MOS2.

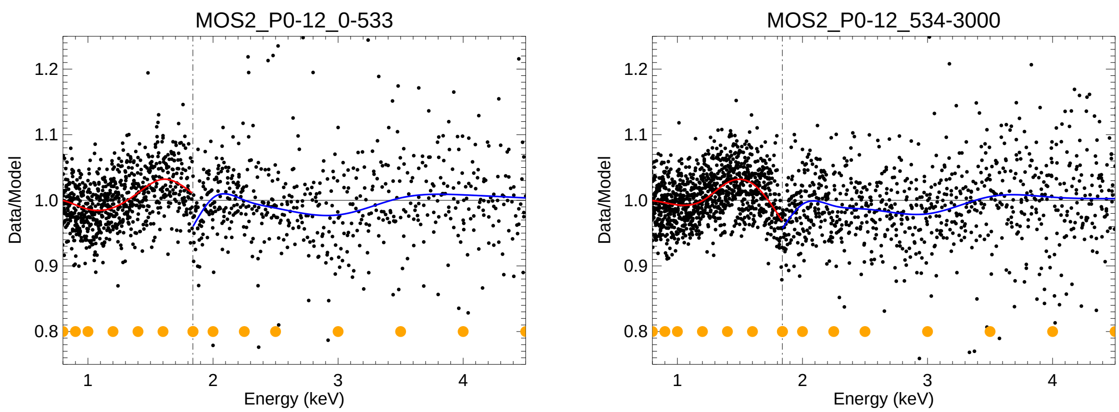

Figure 4: As Figure 2 but for MOS2.

4.2 Tests on the 2XMM sample

The new MOS QE CCF constituents have also been used to generate effective areas for the MOS spectra of the 2XMM sources discussed by Read et al. (2014). We extracted their spectra with SASv13.5 and associated calibration files, which include the calibration of the time-dependent contamination affecting the EPIC-MOS effective area (Sembay & Saxton 2013). Fig. 6 shows the stacked residuals in the 0.9–2.2 keV energy range generated using the same technique as discussed in Sect. 4.1. Taking into account the lower statistical quality of this sample, the application of the new CCFs yields a comparable improvement in the quality of the fit around the energy of the Silicon edge, with a possible exception of a single data point at $\simeq$1.9 keV in EPIC-MOS1. The residual systematic uncertainties on the effective area at the Silicon edge as measured on this sample are $\pm$1% and $\pm$0.75% in MOS1 and MOS2, respectively. Investigation on the telescope effective area calibration is ongoing (Lumb et al., in preparation).

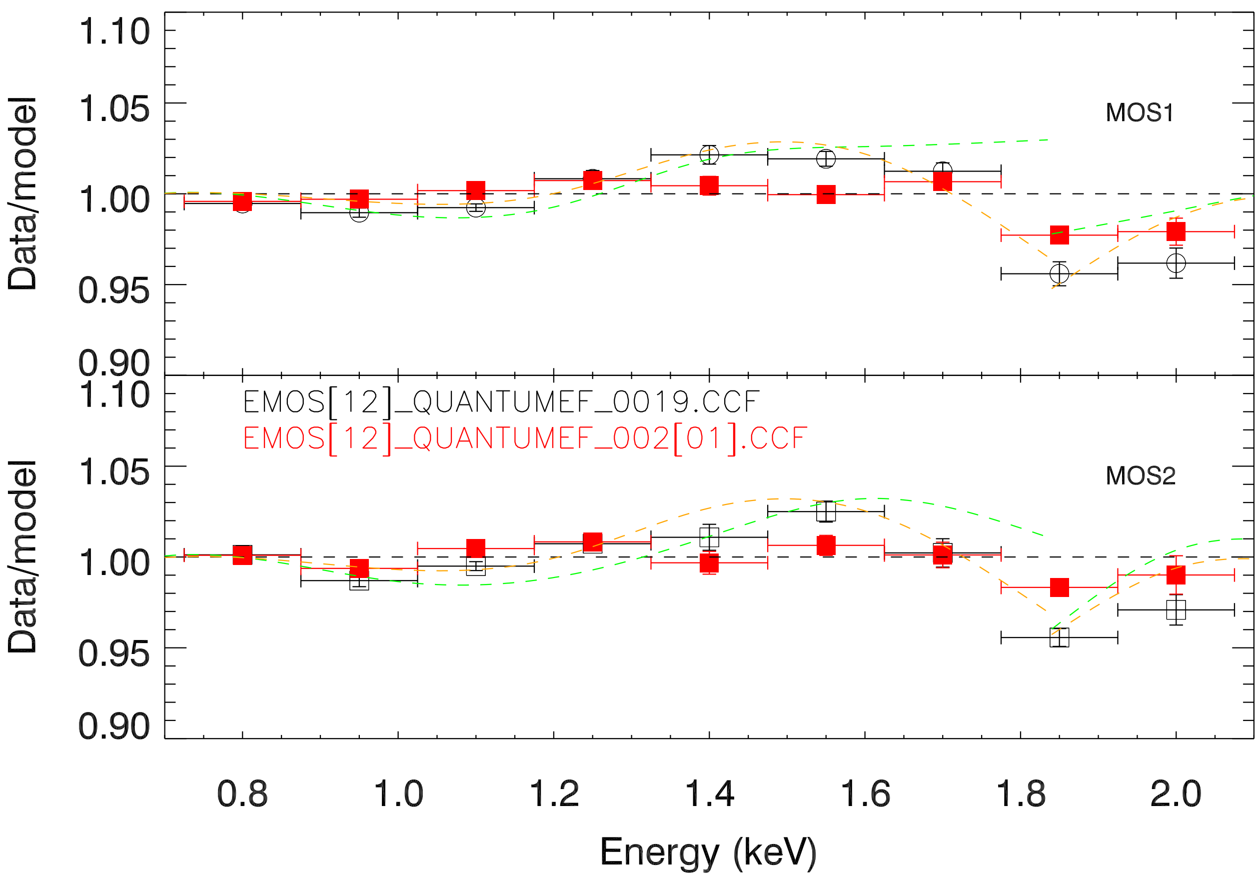

Figure 5: Stacked residuals in the 0.9–2.2 keV energy band for the sources labelled as "Yes" in Table 1. *Black*: `EMOS[12]_QUANTUMEF_0019.CCF`; *red*: `EMOS[12]_QUANTUMEF_002[01].CCF`. The *dashed lines* indicate the best-fits in Figs. 2 and 4 for the orbit ranges before (*green*) and after (*orange*) the camera cooling. Error bars are at the 1σ level.

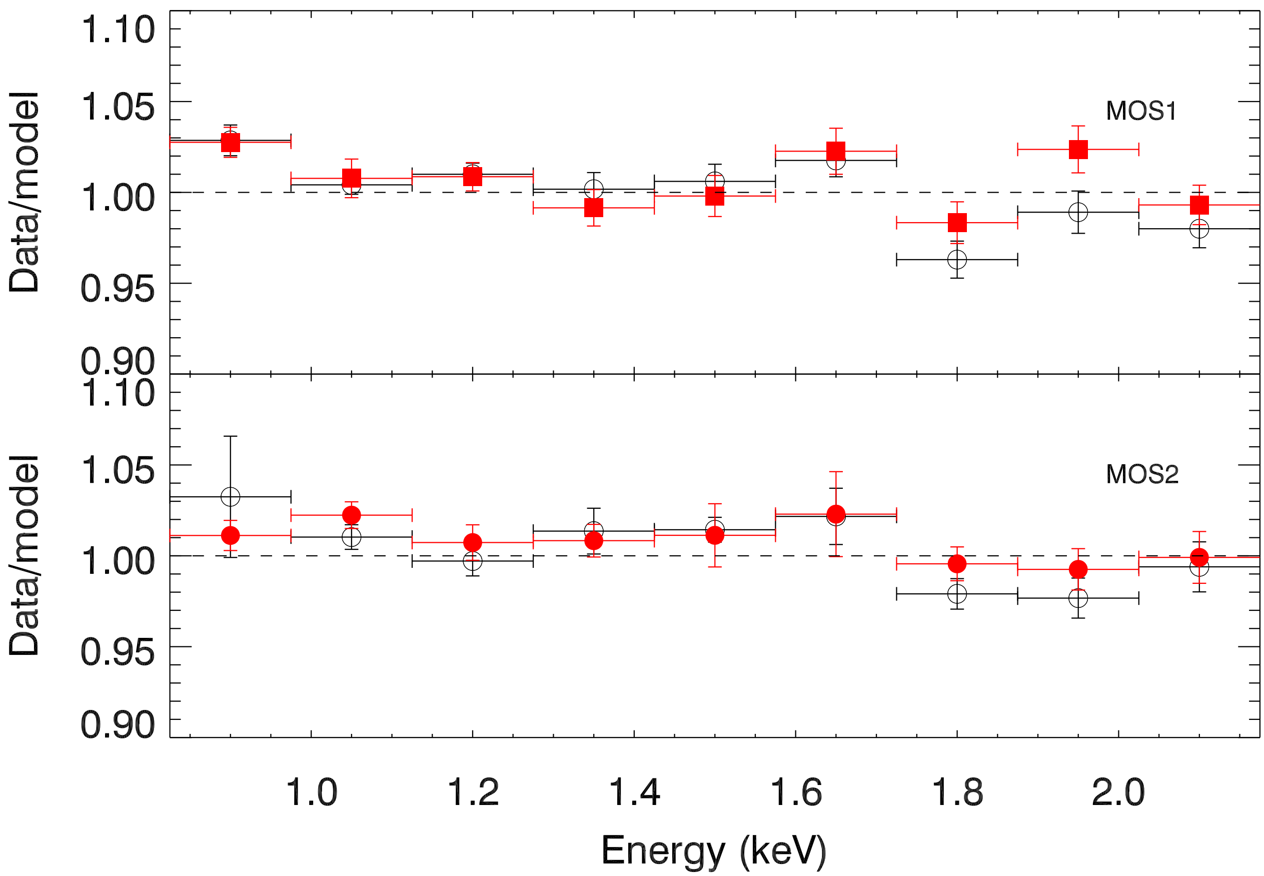

Figure 6: The same as Fig. 5 for the 2XMM sample after Read et al. (2014). The best-fit calibration lines are not shown here for clarity.

5 Expected updates

No further updates of the EPIC-MOS Quantum Efficiency calibration are expected in the nearby future.

References

Kettula K., et al., 2013, A&A, 552, 47

Longinotti A., et al., 2008, RMXAC, 32, 62

Read A., et al., 2014, A&A, 564, 75

Sembay S. & Saxton R., 2013, XMM-CCF-REL-305 (available at: `http://xmm2.esac.esa.int/docs/documents/CAL-SRN-0305-1-0.ps.gz`)

Stuhlinger M., et al., 2010, XMM-CAL-TN-0052 (available at: `http://xmm2.esac.esa.int/docs/documents/CAL-TN-0052.ps.gz`)